

EU contract number RII3-CT-2003-506395

CARE Conf-04-039-PHIN



### **Electrons and protons beam produced by ultra short laser pulses**

V. Malka, J.Faure, S. Fritzler, and Y. Glinec

*Laboratoire d'Optique Appliquée – ENSTA, CNRS UMR 7639, Ecole Polytechnique,  
Chemin de la Lumière, 91761 Palaiseau, France*

#### **Abstract**

It is known that relativistic laser plasma interactions can induce accelerating fields beyond one TV/m. Such electric fields are capable of efficiently accelerating plasma background electrons as well as protons. Depending on the target medium, high quality particle beams can be generated. An introduction to the current state of the art will be given and possible applications of these optically induced charged particle beams will be discussed.

Contribution to the Laser and Nuclei Workshop, 2004

Work supported by the European Community-Research Infrastructure Activity under the FP6 «Structuring the European Research Area » programme (CARE, contract number RII3-CT-2003-506395).

# Electrons and protons beam produced by ultra short laser pulses

V. Malka, J.Faure, S. Fritzler, and Y. Glinec

*Laboratoire d'Optique Appliquée – ENSTA, CNRS UMR 7639, Ecole Polytechnique,*

*Chemin de la Humière, 91761 Palaiseau, France*

It is known that relativistic laser plasma interactions can induce accelerating fields beyond one TV/m. Such electric fields are capable of efficiently accelerating plasma background electrons as well as protons. Depending on the target medium, high quality particle beams can be generated. An introduction to the current state of the art will be given and possible applications of these optically induced charged particle beams will be discussed.

## I. Introduction

Since their discovery, beams of particles like electron and proton beams have been of great interest and relevance in various scientific domains. The evolution of the quality of these beams, by extending one of their properties (like emittance, bunch length, or energetic distribution), is always associated to new investigations and sometimes to new discovery. For example, a higher luminosity is obviously preferential for high energy physics experiments where the number of events for a given phenomenon is very small. Similarly, shorter particle bunches permit the investigation of phenomena with higher temporal resolution. For high resolution radiography experiments, the electron beam should have a small, point-like source in order to enhance the resolution. This can be achieved with high quality beams with low emittances. Finally a reduction of the size of accelerators can reduce the total cost since it corresponds directly to a reduction of the cost of the infrastructure.

Today, the most efficient pulsed electron sources are photo-injector guns, where lasers with energies of some tens of  $\mu\text{J}$  and pulse durations of some ps irradiate cathodes and liberate electrons. However, in this case, these lasers are not intended to accelerate electrons to high energies. With the advent of the Chirped Pulse Amplification (CPA) [1], high power, sub-ps laser pulses have become available. Focusing such lasers down to focal waists of some  $\mu\text{m}$  and intensities beyond  $10^{18}$  W/cm<sup>2</sup>, intrinsic electric fields of several TV/m can be obtained. At such high intensities, these lasers can create quasi-instantaneously plasmas on the targets they are focused onto, i.e., they generate a medium consisting of free ions and electrons. Inside this plasma, the transverse electric laser fields can be turned into longitudinal plasma electron oscillations, known as plasma waves, which are indeed suitable for electron acceleration [2]. Additionally, due to the high laser intensity, strong quasi-static electric fields can be induced, which are capable of subsequently accelerating ions.

In this article, we will give a brief overview on the theoretical aspects of charged particle generation induced by relativistic laser-plasma interactions. Recent experiments on electron as well as proton generation will be described and an outlook on near-future experiments will be given. Finally, possible applications of these charged particle sources will be discussed.

## II. Theoretical background

### II. A) Electron beam generation in underdense plasmas :

Electron beams can be generated by the breaking of relativistic plasma waves in an underdense plasma (plasma with an electron density below the critical density,  $n_e < n_c$ , this condition is necessary for allowing the laser to propagate in the plasma). For a laser with power exceeding few tens of TW propagating in a plasma with density values higher than a few  $10^{18} \text{cm}^{-3}$ , more precisely for laser and plasma parameters satisfying  $P_L/P_c > \text{few unit}$  ( $P_L$  is the laser power and the  $P_c(\text{GW})=17 n_c/n_e$ , the critical power for relativistic self focusing), relativistic plasma waves can be excited, reaching the wave breaking limit which permits the generation of an energetic, collimated and forward propagating electron beam. These electron beams were initially demonstrated using an energetic laser beam working in the ps range at low repetition rate (one shot/20 min) [3]. But these beams are now currently being produced with shorter laser pulses for which the required energy is considerably reduced, allowing laser plasma accelerators to work with a 10 Hz repetition rate. Using 10 Hz, 100 fs laser, electron beam with energy up to 10 MeV have been accelerated directly by the laser (DLA) [4], whereas using 10 Hz, 30 fs at lower electron density, 70 MeV energies have been reach due to an efficient acceleration by plasma waves [5]. This is illustrated on Figure 1: the maximum electron energy increases when the phase velocity of plasma wave increases (i.e. when the electron density decreases). In addition, the continuous line indicates that for densities below  $10^{19} \text{cm}^{-3}$ , the expected value of the gain is well below the theoretical one. This is because of (i) very intense radial electric field and (ii) a Rayleigh length shorter than the dephasing length can limit the optimum gain. To overcome this problem, longer laser plasma interaction lengths are needed. They can be achieved by using a lower optic aperture or by using a plasma channel. Using a long off-axis parabola, a 30 fs laser pulse propagating at very low density can excite plasma waves with amplitudes corresponding to a highly non linear regime of great interest for the production of good quality electron beams [6]. Normalized emittance was found to be as low as  $(2.7 \pm 0.9) \pi \text{ mm mrad}$  for  $(54 \pm 1) \text{ MeV}$  electrons [7]. At densities even lower, for which laser pulse length  $c\tau_L$ , is smaller than the plasma wavelength  $\lambda_p$ , electrons beams with prodigious parameters have recently been produced [8].

In the forced laser wakefield (FLWF) regime, occurring when  $P_L > P_c$  and  $c\tau_L \approx \lambda_p$ , non-linear interaction can excite non linear plasma waves when propagating over long enough distances. Using these conditions, a combination of laser beam self-focusing, front edge laser pulse steepening and relativistic lengthening of the plasma wave wavelength can result in a forced growth of the wakefield plasma wave [6,9]. Since in the FLWF regime the interaction of the bunch of accelerated electrons with the laser is reduced, this can yield the highest known electron energy gains attainable with laser plasma interactions. Since the laser interaction with the plasma wave and with the electron beam is reduced, the generated electron beam has a very good spatial quality with an emittance as good as those obtained in conventional accelerators.

Using the same laser (pulse duration, laser energy and focusing aperture), by carefully scan the electron density, we observe a monoenergetic feature in the electron distribution in agreement with 3D PIC simulations performed by Prof. A. Pukhov and Prof. J. Meyer-Ter-Vehn, in a new ‘light bullet regime’ [10]. During its propagation in the underdense plasma, the laser excites relativistic plasma waves, since its power exceed the one for self focusing, the laser radius is reduced by a factor of three, producing a laser beam with parameters well adapted to excite resonantly a non linear plasma wave. At this point, the laser ponderomotive potential expels the plasma electrons radially and leaves a cavitated region (or ‘plasma bubble’) behind. Electrons from the wall of the bubble are then injected and

accelerated inside the bubble. Since they have a well defined location in phase space they form a high quality electron beam.

## II. B) Proton beam generation in overdense plasmas :

In contrast, proton beams are more efficiently generated in overdense plasmas,  $n_e > n_c$ . Even though the laser beam cannot propagate through the overdense medium, its ponderomotive force accelerates electrons in the plasma skin layer. This force is responsible of two ions acceleration mechanisms : (i) ponderomotive and (ii) plasma sheath acceleration. The ponderomotive force expels the electrons from the high-field regions, setting up a charge imbalance that accelerates the ions in turn. This mechanism includes forward ion acceleration at the surface of an irradiated solid target [11]; it is very sensitive to the state of the surface at the front side as well as to the size of the preplasma. In the second process, plasma sheath acceleration, the forward ion beams properties are more related to the back surface parameters since the electric field components are normal to the surface target. Here the charge imbalance is maintained by heating a fraction of the plasma electrons to a very large temperature. This large electron thermal pressure drives an expansion of these hot electrons, setting-up a large-amplitude electrostatic field when they cross the target-vacuum interface. The accelerated ions detected behind thick targets [12] and the high-energy plasma plume emitted from the laser-irradiated surface [13] come from these ‘plasma sheath acceleration’.

## III. Results on electron beam produced by Non Linear Plasmas Waves.

The very first experiment on the FLW regime was performed on the “salle jaune” laser at *Laboratoire d’Optique Appliquée* (LOA), operating at 10 Hz and a wavelength of 820 nm in the CPA mode. It delivered on target energies of 1 J in 30 fs full width at half maximum (FWHM) linearly polarized pulses, whose contrast ratio was better than  $10^{-6}$  [14] Using a  $f/18$  off-axis parabolic mirror, the laser beam was focused onto the sharp edge of a 3 mm supersonic helium gas jet. Since the focal spot had a waist of 18  $\mu\text{m}$ , this resulted in peak intensities of up to  $3 \times 10^{18}$  W/cm<sup>2</sup>. The characterization of the electron beam was performed using an electron spectrometer, integrating current transformer (ICT), radiochromic film, and nuclear activation techniques. Typical electron beam spectra obtained at around  $2.5 \times 10^{19}$  cm<sup>-3</sup> present a distribution with maxwellian shape (for electron with energies below 120 MeV) with a plateau for more energetic electrons. The total charge of the electron beam was measured to be about 5 nC, determined with a 10 cm diameter ICT, installed 20 cm behind the gas jet nozzle. Subsequently, the electron beam was collimated by a 1 cm internal diameter opening in a 4 cm thick stainless steel piece at the entrance of an electron spectrometer, which gave a collection aperture of  $f/100$ . The electron spectrum was measured with five biased silicon Surfaced Barrier Detectors (SBD) placed in the focal plane of the electron spectrometer. By changing the magnetic field in the spectrometer from 0 to 1.5 T it is possible to measure electrons with energies from 0 to 217 MeV. The angular distribution was measured inserting on the electron beam path a sandwich of radiochromic film and copper foil and by accumulating shots in order to get measurable signal on the film. By decreasing the electron density to lower values we observed a strong saturation of the signal from the diodes measuring high energy electrons. This was an indication that the charge at high energy had tremendously increased and that this spectrometer was no longer adapted for measuring electrons produced in this new regime. Therefore, we changed the design of our spectrometer in order to obtain a complete electron spectrum on a single shot basis and to lower the saturation value.

For energy distribution measurements, a 0.45 Tesla, 5 cm long permanent magnet was inserted between the gas jet and the LANEX screen. The LANEX screen, placed 25 cm

after the gas jet, was protected by a 100  $\mu\text{m}$  thick Aluminium foil in order to avoid direct exposure to the laser light. As electrons passed through the screen, energy was deposited and reemitted into visible photons which were then imaged onto a 16 bit Charged Coupled Device (CCD) camera. The resolution is respectively 32 MeV and 12 MeV for 170 MeV and 100 MeV energies. The charge of the electron beam was measured using an integrating current transformer placed 30 cm behind the LANEX screen. It allowed us to measure the total charge of the beam when no magnetic field was applied, and the charge above 100 MeV when the magnetic field was applied. This experimental improvement has permit to observe, in a very narrow electron density range centered at  $7.5 \times 10^{18} \text{cm}^{-3}$  an highly charged, 500 pC monoenergetic component at 170 MeV in the electron energy distribution ( $170 \pm 20$  MeV) as it was predicted by numerical simulations.

#### **IV. Proton beam generation with solid targets**

As already mentioned above, the same laser can be used to generate proton beams when shooting it onto overdense plasmas, for example using solid targets. Here, the laser with an on target energy of up to 840 mJ and a FWHM duration of 40 fs was focused using a  $f/3$  off-axis parabolic mirror. Since the focal waist was 4  $\mu\text{m}$ , this resulted in peak intensities of up to  $6 \times 10^{19} \text{W/cm}^2$ . For these pulses, the laser contrast ratio was, again, found to be of the order of  $10^{-6}$ . The target, a metallic aluminium foil of 6  $\mu\text{m}$  thickness, was irradiated by the laser at normal incidence.

The energy, yield as well as the opening cone of generated protons were determined with CR-39 nuclear track detectors, which were partially covered with aluminium foils of varying thicknesses, which served as energy filters.

Figure 5 shows the measured proton energy distribution. Clearly, the energy of this beam reaches 10 MeV.

#### **V. Perspectives :**

Electron beams produced by laser do not have the same properties than beams produced in conventional accelerators. As such, they offer some complementary applications of great interest in several domains. For example, standard accelerators typically provide energetic electron bunches with a bunch duration in the ps range and an energy resolution of less than  $10^{-3}$ . To achieve these performances, such devices are precisely designed and, hence, for a fixed electron energy only. Even though this high energy resolution is not met in the laser plasma accelerators approach, this approach will permit to generate tunable, energetic, high charge and high quality electron beams with an extremely short duration. The shortness of the electron bunches has recently permitted to obtain interesting results on ultra-fast radiation chemistry. In this pump-probe experiment, the sub-ps electron bunch was propagating through a suprasil cell containing pure liquid water producing radiolytic events. For the first time, it was probed in the sub-ps regime at LOA [15] by using a laser probe beam free of jitter. Taking benefit of the high spatial quality of the beam has permitted to radiograph a dense matter object with spatial resolution of less than 400 microns [16]. This was achieved by generating a point-like gamma-ray source by bremsstrahlung radiation.

Proton accelerators also produce beams with properties different from the ones produced with lasers. Even though today, the energy spectrum of this proton beam has a broad Maxwellian-like distribution, it can nevertheless be interesting for the generation of Positron Emission Tomography (PET) radio-isotopes since its energy is greater than the  $Q$ -

value (few MeV for  $(p,n)$  reactions of most prominent isotopes). Calculating the expected PET isotopes activity after an irradiation time of 30 min and a repetition rate of 1 kHz, which is indeed feasible in the very near future, activities of the order of 1 GBq can be obtained for  $^{11}\text{B}$  and  $^{18}\text{O}$ , which are required in order to separate the tracer from the inactive carrier with fast chemistry techniques [17]. Interestingly, numerical simulations indicate that a modest increase in laser intensity to  $8 \times 10^{19}$  W/cm<sup>2</sup> can result in even more protons at higher energies and can lead to a sevenfold increase in  $^{18}\text{F}$  activity.

Another very interesting challenge concerns the use of optically induced proton beams for proton-therapy. Some groups have already started to investigate this approach on the basis of numerical simulations and have shown that implementing a PW laser with a pulse duration of 30 fs and a repetition rate of 10 Hz will indeed meet the requirements for this purpose [18-20] as the dose delivered with such an adjustable proton beam spectrum within the therapeutic window (in between 60 and 200 MeV) is already expected to be beyond some few Gy/min. Importantly this approach could provide a double benefit : (i) the size and weight of the facility is reduced, allowing a possible installation inside standard radiotherapy departments and reducing significantly the costs, (ii) as the main beam in this “accelerator” is a laser beam, whilst proton generation only occurs at the end, one could also expect to reduce the size and weight of the gantries and of the associated radiation shielding [21].

## V. Conclusions

In summary the above mentioned approach on optically induced particle beams have some very interesting features: (i) their accelerating field gradients are by 4 orders of magnitude higher than those attainable with today’s standard techniques, which can consequently cut down significantly the accelerating length; (ii) the required lasers are rather compact and could become cheap in the future compared to current RF-structures; (iii) no shielding for radioprotection is required up to the point where the laser creates a plasma on the target; (iv) the same laser can be used to generate electrons or protons simultaneously; (v) the particle beams generated are of very good quality, with emittance values better than the one obtained with conventional accelerators, (vi) the particle bunches are ultra short (durations can be less than few tens of fs), and (vii) they will be tunable.

## VI. Acknowledgements

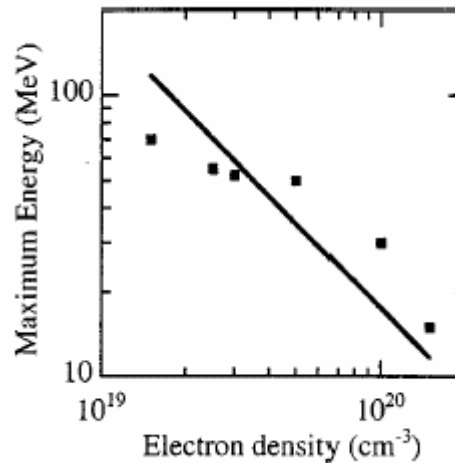
The authors greatly appreciate the support and the quality of the “salle jaune” laser, which was ensured by the entire LOA staff. Some of the experimental data on electrons have been obtained in collaboration with Imperial College and with LULI and on protons in collaboration with University of Strathclyde. Additionally, we are indebted to the fruitful discussions with E. Lefebvre of CEA, A. Pukhov of ITP, and P. Mora of CPhT on theoretical issues. We also acknowledge the support of the European Community Research Infrastructure Activity under the FP6 "Structuring the European Research Area" program (CARE, contract number RII3-CT-2003-506395).

## REFERENCES

- [1] D. Strickland and G. Mourou, *Optics Comm.* **56**, 219 (1985).
- [2] T. Tajima and J. Dawson, *Phys. Rev. Lett.* **43**, 267 (1979).
- [3] A. Modena, et al., *Nature* **377**, 606 (1995).
- [4] C. Gahn, et al., *Phys. Rev. Lett.* **83**, 4772 (1999).
- [5] V. Malka, et al., *Phys. Plasmas* **8**, 2605 (2001).
- [6] V. Malka, et al., *Science* **22**, Vol.**298**, Nov. (2002).
- [7] S. Fritzler, et al., *Phys. Rev. Lett.* (2004).
- [8] J. Faure, et al., *Nature* **431** (2004).
- [9] Z. Najmudin, et al., *Phys. Of Plasmas* **10**, 15 (2003).
- [10] A. Pukhov, and J. Meyer-Ter-Vehn, *Appl. Phys. B* **74** (2002).
- [11] S. C. Wilks, et al., *Phys. Rev. Lett.* **69**, 1383 (1992).
- [12] R. A. Snavely, et al., *Phys. Rev. Lett.* **85**, 2945 (2000).
- [13] E. L. Clark, et al., *Phys. Rev. Lett.* **84**, 670 (2000).
- [14] M. Pittman, et al., *Appl. Physics B*. **74**, 529 (2002).
- [15] Y. Gauduel, et al., Submitted To *Phys. Chem.*
- [16] Y. Glinec, et al., Submitted to *Phys. Rev. Lett.*
- [17] S. Fritzler, et al., *Appl. Phys. Lett.* **83**, 15 (2003).
- [18] S. V. Bulanov and V. S. Khoroshkov, *Plasma Phys. Rep.* **28**, 5 (2002).
- [19] E. Fourkal, et al., *Med. Phys.* **29**, 12 (2002).
- [20] E. Fourkal, et al., *Med. Phys.* **30**, 7 (2003).
- [21] V. Malka, et al., *Medical Physics* **31**, **6**, June (2004).

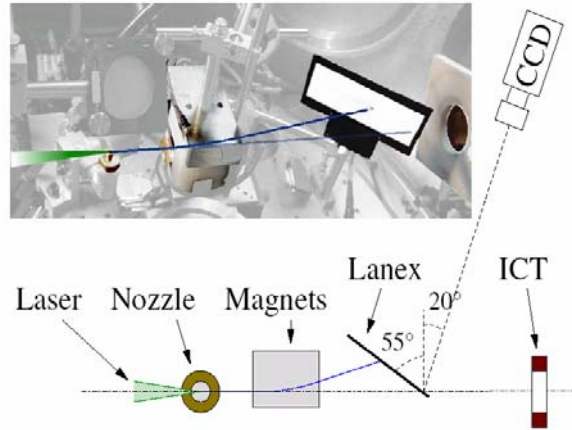
## FIGURE CAPTIONS

Figure 1 :



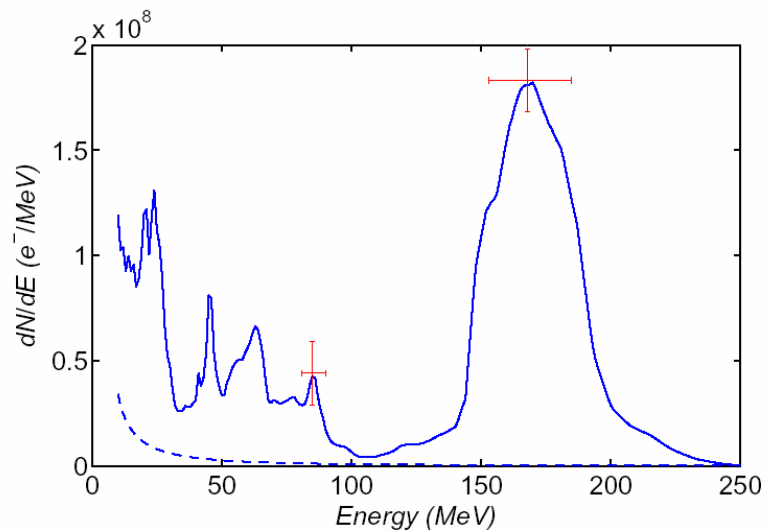
Maximum electron energy obtained with a 30 cm off axis parabola with a 0.6 J laser energy, 35 fs laser pulse focused down a 6  $\mu\text{m}$  focal spot (laser intensity about  $2 \cdot 10^{19} \text{ W/cm}^2$ ) as a function of the electron density. The theoretical value deduced from the linear theory  $W_{\text{max}} \approx 4\gamma_p^2(E_z/E_0)mc^2$ , where  $\gamma_p$  is the plasma wave Lorentz factor has been plot for  $E_z/E_0 = 0.5$ , where  $E_z/E_0$  is the electrostatic field normalized to  $E_0 = c m \omega_p / e$ .

Figure 2 :



Experimental set-up with the compact device for single shot electron distribution. Top: picture from the experiment, bottom: schematic. The laser beam is focused onto a 3 mm supersonic gas jet and produces a very collimated electron beam whose spectra is measured using the compact magnet with a LANEX scintillator screen and an ICT.

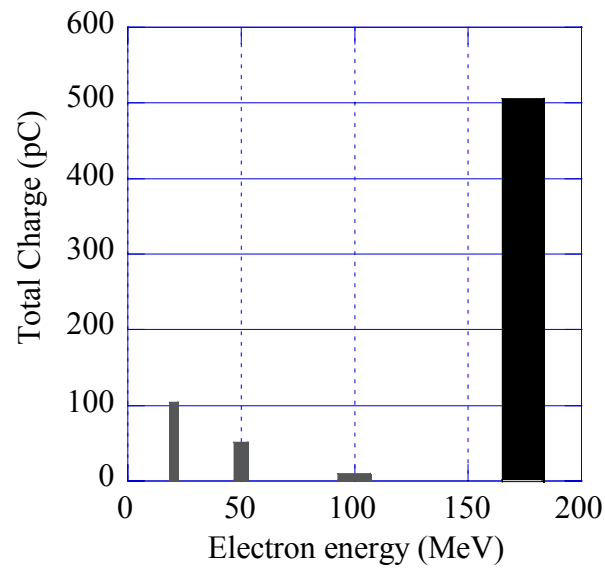
Figure 3 :



Corresponding electron spectrum obtained at  $7.5 \times 10^{18} \text{ cm}^{-3}$ . The dashed line represents an estimation of the background level. The red horizontal error bars indicate the resolution of the spectrometer.

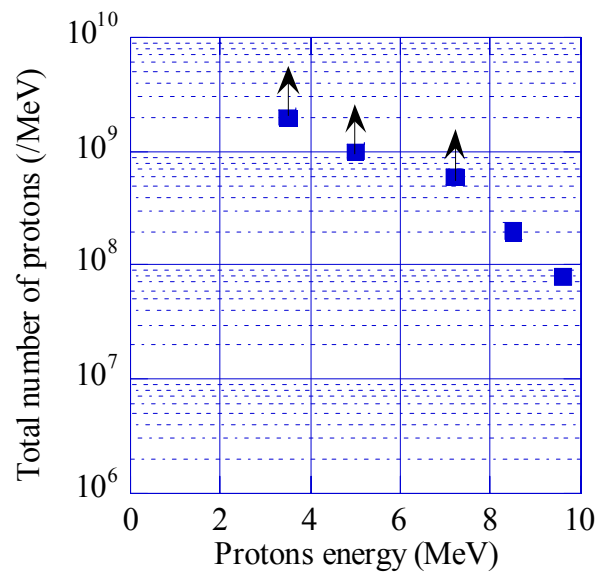


Figure 4 :



Charge in a 10 % energy bandwidth obtained at  $2 \times 10^{19}$  (in gray) and  $7.5 \times 10^{19} \text{ cm}^{-3}$  (in black). Note the 3 orders of magnitude increased for electron energy around 175 MeV.

Figure 5 :



Proton energy spectra at a laser irradiance of  $6 \times 10^{19} \text{ W/cm}^2$  for a  $6 \mu\text{m}$  aluminium target. The arrow indicates the minimum number of protons, which results of the saturation of the detectors.